Polarisation observations of VY Canis Majoris H2O 5(32)-4(41) 620.701 GHz maser emission with HIFI

Harwit, M.; Houde, M.; Sonnentrucker, P.; Boogert, A.C.A.; Cernicharo, J.; De Beck, E.; Decin, L.; Henkel, C.; Higgins, R.D.; Jellema, W.; Kraus, A.; McCoey, C.; Melnick, G.J.; Menten, K.M.; Risacher, C.; Teyssier, D.; Vaillancourt, J.E.; Alcolea, J.; Bujarrabal, V.; Dominik, C.; Justtanont, K.; de Koter, A.; Marston, A.P.; Olofsson, H.; Planesas, P.; Schmidt, M.; Schöier, F.L.; Szczerba, R.; Waters, L.B.F.M.

DOI
10.1051/0004-6361/201015042

Publication date
2010

Document Version
Final published version

Published in
Astronomy & Astrophysics

A&A 521, L51 (2010)
DOI: 10.1051/0004-6361/201015042

Astronomy & Astrophysics

Polarisation observations of VY Canis Majoris H_2O 5_{32}–4_{41} 620.701 GHz maser emission with HIFI⋆,⋆⋆

M. Harwit[1], M. Houde[2], P. Sonnentrucker[3], A. C. A. Boogert[4], J. Cernicharo[5], E. de Beck[6], L. Decin[6,16], C. Henkel[7], R. D. Higgins[8], W. Jellema[9], A. Kraus[7], C. M^{c}Coey[10,2], G. J. Melnick[11], K. M. Menten[7], C. Risacher[9], D. Teyssier[12], J. E. Vaillancourt[13], J. Alcolea[14], V. Bujarrabal[15], C. Dominik[16,17], K. Justtanont[18], A. de Koter[16,19], A. P. Marston[12], H. Olofsson[18,20], P. Planesas[15,21], M. Schmidt[22], F. L. Schöier[18], R. Szczerba[22], and L. B. F. M. Waters[6,16]

(Affiliations are available on page 5 of the online edition)

Received 26 May 2010 / Accepted 3 September 2010

ABSTRACT

Context. Water vapour maser emission from evolved oxygen-rich stars remains poorly understood. Additional observations, including polarisation studies and simultaneous observation of different maser transitions may ultimately lead to greater insight.

Aims. We have aimed to elucidate the nature and structure of the VY CMa water vapour masers in part by observationally testing a theoretical prediction of the relative strengths of the 620.701 GHz and the 22.235 GHz maser components of ortho H_2O.

Methods. In its high-resolution mode (HRS) the *Herschel* Heterodyne Instrument for the Far Infrared (HIFI) offers a frequency resolution of 0.125 MHz, corresponding to a line-of-sight velocity of 0.06 km s^{-1}, which we employed to obtain the strength and linear polarisation of maser spikes in the spectrum of VY CMa at 620.701 GHz. Simultaneous ground based observations of the 22.235 GHz maser with the Max-Planck-Institut für Radioastronomie 100-m telescope at Effelsberg, provided a ratio of 620.701 GHz to 22.235 GHz emission.

Results. We report the first astronomical detection to date of H_2O maser emission at 620.701 GHz. In VY CMa both the 620.701 and the 22.235 GHz polarisation are weak. At 620.701 GHz the maser peaks are superposed on what appears to be a broad emission component, jointly ejected from the star. We observed the 620.701 GHz emission at two epochs 21 days apart, both to measure the potential direction of linearly polarised maser components and to obtain a measure of the longevity of these components. Although we do not detect significant polarisation levels in the core of the line, they rise up to approximately 6% in its wings.

Key words. stars: AGB and post-AGB – stars: winds, outflows – supergiants – circumstellar matter – masers – reference systems

1. Introduction

VY Canis Majoris is a highly luminous, strongly obscured, variable supergiant with a high infrared excess. Only ∼1% of the total luminosity is observed at optical wavelengths. The star's distance has been measured to be $D = 1.1$ kpc (Choi et al. 2008) implying a luminosity $L = 3 \times 10^5\ L_\odot$ (Menten et al. 2008). Three thermally emitted mid-infrared water vapour emission lines seen in spectra obtained with the short wavelength spectrometer (SWS) on ISO indicate a mean radial velocity of order 20 ± 2 km s^{-1} and a 25 km s^{-1} H_2O outflow velocity (Neufeld et al. 1999), significantly lower than the 32 km s^{-1} velocities that Reid & Muhleman (1978) reported for 1612 MHz OH maser outflow.

The effective temperature of the central star, $T_* = 2800$ K (Monnier et al. 1999), combined with distance and inferred luminosity fixes the star's radius at $R_* \sim 10$ AU. Working at 11 μm, Danchi et al. (1994) reported a variable photospheric radius ranging from 9.5 to 11 mas, where 10 mas corresponds to a stellar radius of 10 AU.

VY CMa is a strong source of 6_{16}–5_{23} 22.235 GHz water vapour maser emission. Recent observations at the Atacama Pathfinder EXperiment (APEX) telescope have revealed H_2O maser emission also at eight submillimetre frequencies, ranging from 321 to 475 GHz (Menten et al. 2008). Although a theoretical model of Neufeld & Melnick (1991) predicted that the 22.235 GHz transition should be far more luminous than these submillimetre transitions, Menten et al. (2008) find them to be comparable in flux density, or at most a factor of ∼6 lower. This suggests a need for further observations that might explain the discrepancies.

One of strongest submillimetre masers predicted by Neufeld & Melnick (1991) is due to the 5_{32}–4_{41} 620.701 GHz transition of ortho water, whose photon luminosity was expected to be roughly 16% that of the 22.235 GHz maser. Given the multiple masers observed at 22.235 GHz we expected the 620.701 GHz maser of VY CMa to exhibit similar multiple peaks at photon densities ∼16% of those exhibited at 22.235 GHz.

2. HIFI observations at 620.701 GHz

The *Herschel* Heterodyne Instrument for the Far Infrared (HIFI) covers seven frequency bands, ranging from 488.1 to 1901.8 GHz (de Graauw et al. 2010). The 620.701 GHz radiation of the 5_{32}–4_{41} maser of ortho H_2O is observed in HIFI's Band 1B, which nominally covers the range from 562.6 to 628.4 GHz. Two channels cover each of the frequency bands, one sensitive to linearly polarised radiation roughly parallel to the spacecraft horizontal (H) direction, the other roughly parallel to the vertical direction (V). For Band 1B the H direction of polarisation is at an angle of 82.5° relative to the spacecraft V axis, while the V direction of polarisation is at an angle of –7.5° to that axis. Our data were obtained in the HIFI high-resolution spectroscopy (HRS) mode with spectral resolution 0.125 MHz, or line-of-sight velocity resolution 0.06 km s^{-1}.

⋆ *Herschel* is an ESA space observatory with science instruments provided by European-led Principal Investigator consortia and with important participation from NASA.

⋆⋆ Appendix (page 5) is only available in electronic form at http://www.aanda.org

The H and V beams on HIFI are not fully coincident. In Band 1B they are separated by ∼19% of the ∼34.4″ full-width-half-power beam diameter; the offset between the two beams is ∼6.6″. VY CMa is a spatially unresolved source at these frequencies (Decin et al. 2006). In our observations the star was positioned half-way between beam centres, i.e., displaced ∼3.3″ relative to the centre of each beam, although a random ∼1.8″ pointing error can slightly increase alignment uncertainty.

In order to determine the orientation on the sky of any observed linear polarisation, a source has to be viewed at least at two different rotation angles relative to the telescope. The *Herschel* Space Observatory (Pilbratt et al. 2010), however, cannot be rotated without producing undesirable thermal drifts. A rotation is best achieved by observing a target at two epochs separated by a number of weeks. The further the target lies above the ecliptic plane, the faster is the rotation produced. In our observations, an interval of three weeks between two sightings of VY CMa resulted in a rotation of the telescope of ∼16° about the line of sight to the star.

We first observed the star on March 21, 2010 in two contiguous segments, lasting 10 139 s apiece, for a total observing time of 5.633 h. The first segment began at 08:48:38.0 UT; the second was started at 11:45:00 UT, 7 min and 23 s after the first had terminated. Our second epoch of observations started at 17:02:33 UT on April 11, 2010 and again ran for 10 139 s or 2.816 h. The system temperature for these observations ranged between approximately 80 K and 100 K with respective RMS noise levels for the first and second sets of observations of 6.1 and 5.3 Jy for the H channel, and 4.3 and 4.5 Jy for the V channel at the resolution of 0.125 MHz.

3. Polarisation analysis of the 620.701 GHz maser components

Linear polarisation measurements are often optimised to determine the Stokes Q and U parameters independently from each other (Li et al. 2008; Hezareh & Houde 2010). If we define four intensity measurements I_φ within the equatorial system with φ set to 0° when pointing north and increasing eastwards, then

$$I = (I_0 + I_{45} + I_{90} + I_{135})/2 \quad (1)$$

$$Q = I_0 - I_{90} \quad (2)$$

$$U = I_{45} - I_{135}. \quad (3)$$

Although the state of linear polarisation is completely defined with these equations, it is also commonly expressed with the polarisation fraction $p = \sqrt{Q^2+U^2}/I$ and angle $\theta = 0.5 \arctan(U/Q)$. Alternatively, we can also write

$$Q = pI\cos(2\theta) \quad (4)$$

$$U = pI\sin(2\theta). \quad (5)$$

With HIFI we do not generally have access to four independent measurements precisely sampled with a spacing of 45°, as in Eqs. (1)–(3). Instead, we may have access to N irregularly spaced observing epochs with the HIFI vertical polarisation axis (V) oriented at an angle φ_i relative to north ($i = 1, 2, \ldots, N$) and the horizontal polarisation axis (H) at $\varphi_i + 90°$, each observation yielding a pair of intensities I_{V_i} and I_{H_i}.

These $2N$ intensities yield the polarisation if we first define

$$d_i \equiv I_{\mathrm{V}_i} - I_{\mathrm{H}_i} = Q\cos(2\varphi_i) + U\sin(2\varphi_i). \quad (6)$$

Introducing a vector d with elements d_i/σ_i, where d_i is the intensity difference of Eq. (6) and σ_i its uncertainty (i.e., the corresponding noise intensity), we can write the matrix equation

$$\mathbf{d} = \mathbf{A}\cdot\mathbf{s}, \quad (7)$$

where the matrix $\mathbf{A}$ and vector s are given by

$$\mathbf{A} = \begin{pmatrix} \cos(2\varphi_1)/\sigma_1 & \sin(2\varphi_1)/\sigma_1 \\ \vdots & \vdots \\ \cos(2\varphi_N)/\sigma_N & \sin(2\varphi_N)/\sigma_N \end{pmatrix} \quad (8)$$

$$s = \begin{pmatrix} Q \\ U \end{pmatrix}. \quad (9)$$

The vector $\mathbf{s}$, and therefore the Stokes parameters, are easily obtained by inverting Eq. (7) using the pseudo-inverse matrix of $\mathbf{A}$. We then find

$$s = \left[\left(\mathbf{A}^T\mathbf{A}\right)^{-1}\mathbf{A}^T\right]\cdot d. \quad (10)$$

The elements of the covariance matrix $\mathbf{C} = \left(\mathbf{A}^T\mathbf{A}\right)^{-1}$ can be shown to yield the corresponding uncertainties on the estimated Stokes parameters with

$$\mathbf{C} = \begin{pmatrix} \sigma_{QQ}^2 & \sigma_{QU}^2 \\ \sigma_{QU}^2 & \sigma_{UU}^2 \end{pmatrix}, \quad (11)$$

where $\sigma_{ij}^2 = \langle s_i s_j\rangle - \langle s_i\rangle\langle s_j\rangle$ with $i, j = Q$ or U and s_i the appropriate component of the vector $\mathbf{s}$. It is also possible to determine the uncertainties σ_p and σ_θ for the polarisation fraction and angle, respectively, with

$$\sigma_p^2 \simeq \frac{1}{p^2I^4}\left(Q^2\sigma_{QQ}^2 + U^2\sigma_{UU}^2 + 2QU\sigma_{QU}^2\right) \quad (12)$$

$$\sigma_\theta^2 \simeq \frac{1}{4p^4I^4}\left(Q^2\sigma_{UU}^2 + U^2\sigma_{QQ}^2 - 2QU\sigma_{QU}^2\right). \quad (13)$$

We have applied this polarisation analysis to our observations of the 620.701 GHz H_2O 5_{32}–4_{41} ortho-transition. Our results shown in Fig. 1 were obtained from the two aforementioned observations made at epochs of corresponding position angles of 261.27° and 277.46°.

Although there are no obvious strong polarisation signals from the maser emission peaks, we clearly detect polarisation levels ranging from $p \simeq 1.5\%$ to $p \simeq 6\%$ in regions of significant line intensity (i.e., from approximately –5 to 45 km s^{-1}). Furthermore, the observed anti-correlation of the polarisation fraction with the Stokes I intensity is similar to previous ground-based polarisation observations (Girart et al. 2004; Hezareh & Houde 2010) aimed at the detection of the Goldreich-Kylafis effect in non-masing molecular lines (Goldreich & Kylafis 1981; Cortes et al. 2005), which appears to have first been detected in evolved stars (Glenn et al. 1997). We will discuss the relevance of the Goldreich-Kylafis effect for our observations in Sect. 7 below.

4. Results

Several instrumental capabilities of HIFI and the observations obtained with them may be noted:

(i) The two orthogonally polarised HIFI receivers are well matched and extremely stable. But observations of extended sources need to be conducted with caution. A slight misalignment of H and V receivers can lead to a "false polarisation" that reverses polarity at half-year intervals (see Appendix A).

(ii) The misalignment of the HIFI receivers does not appear to affect observations of unresolved sources. Our observations realised at two observing epochs indicate that instrumental polarisation, which could be in part due to errors

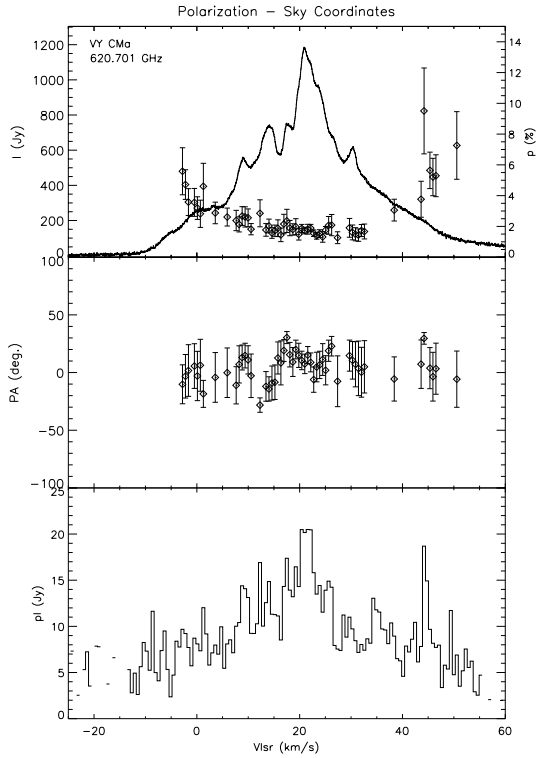

Fig. 1. Polarisation spectrum of the 620.701 GHz H_2O $5_{32}-4_{41}$ ortho-transition for VY-CMa. Shown are, *from top to bottom*, the Stokes I and polarisation fraction (symbols and right axis), the polarization angle, and the (unsigned) polarised flux. The polarisation fraction and flux were corrected for positive bias but not for instrumental polarisation. A simple linear baseline was removed from each V and H channel observation and all polarisation vectors shown satisfy $p \geq 3\sigma_p$ and $I \geq 10\sigma_I$ at the corresponding velocities, where σ_I is the uncertainty (or noise level) on the Stokes I spectrum (i.e., the average of the $I_V + I_H$ spectra measured at the two epochs). The polarisation fraction and angle have their spectral resolution reduced by a factor of 20 compared to Stokes I, which is at the maximum resolution.

in the relative calibration between the two receiver chains of Band 1B, cannot exceed a measure of order 1−2% (see Sect. 7 below).

(iii) The polarisation of VY CMa is not significant near the peak of the 620.701 GHz H_2O $5_{32}-4_{41}$ line, but rises up to ∼6% in the wings of the spectrum in a manner consistent with polarisation due to the Goldreich-Kylafis effect discussed in greater detail in Sect. 7 below.

(iv) The stability of the 620.701 GHz masers is remarkable. The variation over a three week period is $\lesssim$1% (see Fig. 2).

(v) As Fig. 3 shows, the spectral profile of the 620.701 GHz and 22.235 GHz masers appears remarkably similar, except that the relative expansion velocities between peaks, along the line of sight, is a factor of 2.3 greater at 620.701 than for contemporaneous observations at 22.235 GHz (see Appendix B).

(vi) Assuming the 620.701 GHz masers to sit atop a broad pedestal with flux density ∼400 Jy, we find the main 620.701 GHz maser peak flux density to be ∼800 Jy, compared to ∼1900 Jy at 22.235 GHz. The velocity spread of the expanding 620.701 GHz maser peaks is ∼2.3 times wider than at 22.235 GHz, implying a 620.701 GHz photon luminosity roughly 2.4 times lower than at 22.235 GHz – comparable in luminosity to the submillimetre masers observed by Menten et al. (2008), and about 2.5 times more luminous than Neufeld & Melnick (1991) predicted.

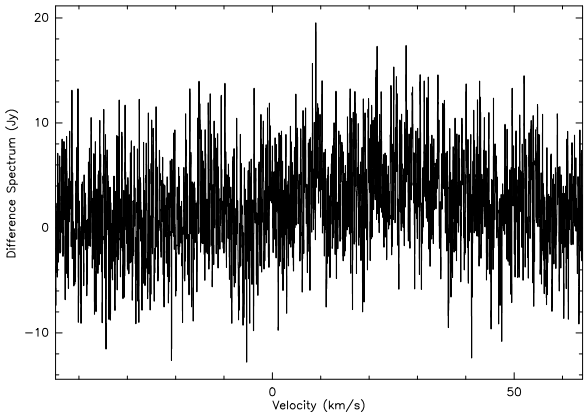

Fig. 2. Residual spectrum resulting from the subtraction of the 620.701 GHz Stokes I spectra taken 3 weeks apart. The residual signal has an amplitude $\lesssim$1%, underlining the accuracy of the relative calibrations as well as the remarkable stability of the masers.

5. Discussion

A spherically symmetric model for the outflows of VY CMa developed by Decin et al. (2006) envisions dust formation in the cooling outflow from the star at distances ∼10 R_*. Radiation pressure then accelerates the dust, and with it also the ambient gas, from velocities $\lesssim$5 km s^{-1} to ∼25 km s^{-1} at a distance of 20 R_*. The kinetic temperature at 20 R_* is of the order of ∼1000 K, sufficient to excite both 620.701 and 22.235 GHz masers. We propose that the masing outflows we observe propagate along several mutually common directions from the star, and that the faster expanding 620.701 GHz masers lie at greater distances from the star than the central cluster of masers peaking at 22.235 GHz. We picture this outflow consisting of gas ejected obliquely to the line of sight to VY CMa but fanning out over a considerable angular width to account for the observed range of outflow velocities. Common ejection of both the denser masing regions and the less-dense ambient medium responsible for the pedestal emission can then account for the observed velocity ranges of both these outflow components. The region from which the 22.235 GHz radiation originates may be at the inner radius of the flow; for, Neufeld & Melnick (1991) find that, for comparable gas densities and H_2O abundances, maser emission at 22.235 GHz should be maximized at line-of-sight velocity gradients ∼30 times lower than those maximizing 620.701 GHz emission.

A comparison of our 620.701 GHz spectrum to the spectra of the star's submillimeter masers observed by Menten et al. (2008) shows that their spectra, observed in June 2006, four years earlier than ours, generally exhibited only two peaks separated by $\lesssim$6 km s^{-1}, whereas our spectrum at 620.701 GHz clearly exhibits four peaks ranging over separations of order ∼25 km s^{-1}. However, their 22.235 GHz spectrum also looks quite different from ours. This is not surprising since Esimbek & Zheng (2001) found that, between August 1993 and August 1999, the shape of the 22.235 GHz spectrum significantly changed and peak emission shifted from $v_{lsr} \sim 17$ to 34.2 km s^{-1}.

Nevertheless, a feature common to all the submillimetre spectra of Menten et al. (2008) is a broad pedestal that diminishes in strength with rising upper-excitation temperature E_u of the observed transitions. For $E_u \sim 725$ K it remains strong with wings extending over a full width $\gtrsim$40 km s^{-1}, whereas at $E_u = 1861$ K, the pedestal has entirely disappeared. The radiation emitted in the pedestal thus appears to be due to collisional excitation by gas flowing out from the star at speeds $\gtrsim$20 km s^{-1}

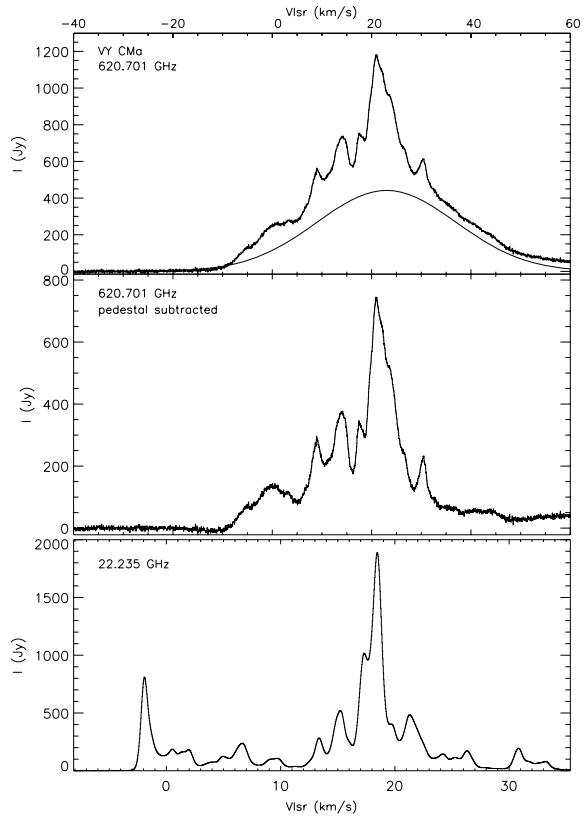

Fig. 3. Comparison of the VY CMa 620.701 and 22.235 GHz masers, both observed on April 11, 2010. The 620.701 GHz (*top*) and the 22.235 GHz (*bottom*) spectra have different velocity scales, and their peaks fall at slightly different $v_{\rm lsr}$ velocities that have been shifted to coincide. Superposed on the 620.701 GHz spectrum is a Gaussian pedestal subtracted in the spectrum just below to display the similarities of the 620.701 and 22.235 GHz maser spectra. Not knowing the source or true shape of the pedestal, we kept its spectrum simple.

close to the terminal velocity in the model of Decin et al. (2006). The pedestal we observe for the transition at 620.701 GHz, whose $E_{\rm u} = 732$ K, has the same broad wings extending roughly symmetrically to either side of the maser outflow peaks.

Low $E_{\rm u}$ levels thus excited can then radiate in three ways, spontaneously, through stimulated emission, or induced by collisions. As Neufeld & Melnick (1991) point out, stimulated emission leads to masing only when the ratio of water vapor density to the velocity gradient along the line of sight is sufficiently high. We interpret the maser peaks in our 620.701 GHz spectrum as emanating from denser clumps in the VY CMa outflow within which the velocity gradient is low, and the 620.701 GHz pedestal as emission from an ambient medium characterized by lower density and/or higher velocity gradients, and thus unable to radiate significantly through stimulated emission to sustain maser amplification. This ambient medium, and its corresponding radiation, will bear the imprint of the Goldreich-Kylafis (GK) effect when also subjected to anisotropic radiation or optical depths, and permeated by a weak magnetic field.

Although the low polarization levels we detect are expected for water masers (Watson 2009), the rise in polarisation seen in the wings of the spectrum in the top panel of Fig. 1 deserves careful consideration. If we assume that the masers simply maser-amplify the seed radiation emanating from the ambient gas responsible for the pedestal component, then we may have a qualitative explanation for the shape of the polarisation spectrum. That is, the polarization fraction should be approximately the same at the position of, and between, maser peaks, as observed in Fig. 1, and should rise in the wings of the line where the optical depth of the pedestal component is lowest, in a manner consistent with the GK effect (Cortes et al. 2005). Although maser-amplification of GK polarisation could lead to different levels of polarisation at the maser peaks, other factors (e.g., magnetic field orientation) could also suppress this effect. We also note that in cases where the pedestal component was highly saturated, the level of polarisation measured in its core would provide a measure of the amount of instrumental polarisation (Hezareh & Houde 2010). Although this scenario probably does not perfectly fit our observations, the polarisation fraction measured in the vicinity of the line core suggests that the instrumental polarisation is approximately 1–2%.

6. Conclusions

We report the first astronomical observations of the 620.701 GHz $5_{32}-4_{41}$ submillimetre maser of ortho H_2O. The maser peaks in VY CMa show weak linear polarisation at levels consistent with the Goldreich-Kylafis effect across the spectral line profile.

Acknowledgements. HIFI has been designed and built by a consortium of institutes and university departments from across Europe, Canada and the United States under the leadership of SRON Netherlands Institute for Space Research, Groningen, The Netherlands and with major contributions from Germany, France and the US. Consortium members are: Canada: CSA, U. Waterloo; France: CESR, LAB, LERMA, IRAM; Germany: KOSMA, MPIfR, MPS; Ireland, NUI Maynooth; Italy: ASI, IFSI-INAF, Osservatorio Astrofisico di Arcetri- INAF; Netherlands: SRON, TUD; Poland: CAMK, CBK; Spain: Observatorio Astronmico Nacional (IGN), Centro de Astrobiología (CSIC-INTA). Sweden: Chalmers University of Technology – MC2, RSS & GARD; Onsala Space Observatory; Swedish National Space Board, Stockholm University – Stockholm Observatory; Switzerland: ETH Zurich, FHNW; USA: Caltech, JPL, NHSC. Support for this work was provided by NASA through an award issued by JPL/Caltech. We thank the HIFISTARS consortium for permission to use their VY CMa 556.9 GHz data for calibration purposes. We would like to acknowledge that Tom Phillips first pointed out to us that HIFI might yield useful polarisation observations. And, finally, we extend thanks to the anonymous referee for perceptive insights and suggestions that greatly improved this paper.

References

Attard, M., Houde, M., Novak, G., & Vaillancourt, J. E. 2008, PASP, 120, 805
Bachiller, R., Pérez Gutiérrez, M., Kumar, M. S. N., & Tafalla, M. 2001, A&A, 372, 899
Choi, Y. K., et al. 2008, PASJ, 20, 1007
Cortes, P. C., Crutcher, R. M., & Watson, W. D. 2005, ApJ, 628, 780
Danchi, W. C., Bester, M., Degiacomi, C. G., Greenhill, L. J., & Townes, C. H. 1994, AJ, 107, 1469
Decin, L., Hony, S., Justtanont, K., Tielens, A. G. G. M., & Waters, L. B. F. M. 2006, A&A, 456, 549
de Graauw, Th., Helmich, F. P., Phillips, T. G., et al., A&A, 518, L6
Esimbek, J., & Zheng, X.-W. 2001, Chin. Phys. Lett., 18, 458
Girart, J. M., Greaves, J. S., Crutcher, R. M., & Lai, S.-P. 2004, Ap&SS, 292, 119
Goldreich, P., & Kylafis, N. 1981, ApJ, 243, L75
Glenn, J., Walker, C. K., Bieging, J. H., & Jewell, P. R. 1997, ApJ, 487, L89
Hezareh, T., & Houde, M. 2010, PASP, 122, 786
Li, H., Dowell, C. D., Kirby, L., Novak, G., & Vaillancourt, J. E. 2008, Appl. Opt., 47, 422
Menten, K. M., Lundgren, A., Belloche, A., Thorwirth, S., & Reid, M. J. 2008, A&A, 477, 185
Monnier, J. D., Geballe, T. R., & Danchi, W. C. 1999, ApJ, 512, 351
Neufeld, D. A., & Melnick, G. J. 1991, ApJ, 368, 215
Neufeld, D. A., Feuchtgruber, H., Harwit, M., & Melnick, G. 1999, ApJ, 517, L147
Pilbratt, G. L., Riedinger, J. R., Passvogel, T., et al. 2010, A&A, 518, L1
Reid, M. J., & Muhleman, D. O. 1978, ApJ, 220, 229
Vlemmings, W. H. T., Diamond, P. J., & van Langevelde, H. J. 2002 A&A, 394, 589
Watson, W. D. 2009, RevMexAA, Conf. Ser., 36, 113

Appendix A: A cautionary note on observations of extended sources

As part of the performance verification of HIFI in space, spectroscopic observations of the $^{12}C^{16}O$ $J = 5 \rightarrow 4$ 576.3 GHz transition were obtained at the position of the chemically-active bow shock B1 driven by the LDN 1157 Class 0 protostar (Bachiller et al. 2001). Initial observations in HIFI's Band 1B were made on August 1, 2009; a second set was obtained 186 days later on February 4, 2010. The spectral shape of the source remained essentially unchanged but initially the signal from the high-frequency edge of the line appeared stronger in the V direction, when the H and V peaks were matched, whereas half a year later it appeared stronger by the same ratio in the H direction.

This "false polarisation" effect was due to the small misalignment of the H and V beams described earlier, which imaged slightly different portions of a scene onto the two receivers (Attard et al. 2008). Unless otherwise specified, observations of a targeted source are centred on a position halfway between the two beam centres. Because the viewing direction of *Herschel* at all times is constrained by the need to keep the plane of the sun-shield roughly perpendicular to the radius vector to the Sun, sources close to the ecliptic plane can only be viewed at half year intervals. Over this interval the telescope aperture rotates 180° about its viewing direction on the sky. Thus, portions of LDN 1157 B1 initially viewed by the V channel were viewed, half a year later, by the H channel and vice versa. It is clear that this effect was not due to linear polarisation because a 180° rotation of the telescope leaves the polarisation direction unchanged.

For VY CMa, where the entire source was relatively well centred on each beam, this effect was negligible. But for linear polarisation observations of an extended source the best strategy may be to make a small map with HIFI over the area of interest, where the spectra obtained in the H and V channels at each position of the source, can be individually and directly compared.

Appendix B: Ground-based observations at 22.235 GHz

Overlapping with the second epoch of 620.701 GHz observations, we observed the VY CMa 22.235 GHz maser with the Effelsberg 100-m telescope of the Max-Planck-Institut für Radioastronomie. Those observations were begun on April 11, 2010 at 16:40 UT and lasted until 17:20 UT and are shown in Fig. 3. Data in two linear polarisations were obtained with the two channels of the *K*-band or 1.3 cm receiver at the primary focus. The frequency resolution was 6.104 kHz, corresponding to a velocity resolution of 0.082 km s^{-1}. Although these observations were realised at only one epoch and are, therefore, insufficient for a full characterisation of the linear polarisation state, a search by Vlemmings et al. (2002) found that the linear polarisation of the VY CMa 22.235 GHz masers is well below 1%.

[1] Cornell University, Center for Radiophysics & Space Research, 511 H street, SW, Washington, DC 20024-2725, USA
e-mail: harwit@verizon.net
[2] University of Western Ontario, Department of Physics and Astronomy, London, Ontario, N6A 3K7, Canada
e-mail: houde@astro.uwo.ca
[3] Johns Hopkins University, Department of Physics and Astronomy, Baltimore, MD 21218, USA
[4] IPAC, Caltech, Pasadena, CA 91925, USA
[5] Consejo Superior de Investigaciones Cientificas, 28006 Madrid, Spain
[6] Katolieke Universiteit Leuven, Institut voor Sterrenkunde, Heverlee 3001, Belgium
[7] Max-Planck-Institut für Radioastronomie, Auf dem Hügel 69, 53121 Bonn, Germany
[8] National University of Ireland, Maynooth, Department of Experimental Physics, County Kildare, Ireland
[9] Space Research Organization of the Netherlands (SRON), 9700 AV Groningen, The Netherlands
[10] University of Waterloo, Department of Physics and Astronomy, Waterloo, Ontario, N2L 3G1, Canada
[11] Harvard-Smithsonian Center for Astrophysics Cambridge, MA 02138, USA
[12] European Space Astronomy Centre, Urb. Villafranca del Castillo, PO Box 50727, 28080 Madrid, Spain
[13] SOFIA Science Center, Universities Space Research Association, NASA Ames Research Center, Moffett Field, CA 94035-0001, USA
[14] Observatorio Astronómico Nacional (IGN), Alfonso XII N°3, 28014 Madrid, Spain
[15] Observatorio Astronómico Nacional (IGN), Ap 112, 28803 Alcalá de Henares, Spain
[16] Sterrenkundig Instituut Anton Pannekoek, University of Amsterdam, Science Park 904, 1098 Amsterdam, The Netherlands
[17] Department of Astrophysics/IMAPP, Radboud University Nijmegen, Nijmegen, The Netherlands
[18] Onsala Space Observatory, Dept. of Radio and Space Science, Chalmers University of Technology, 43992 Onsala, Sweden
[19] The Netherlands and Astronomical Institute, Utrecht University, Princetonplein 5, 3584 CC Utrecht, The Netherlands
[20] Department of Astronomy, AlbaNova University Center, Stockholm University, 10691 Stockholm, Sweden
[21] Joint ALMA Observatory, El Golf 40, Las Condes, Santiago, Chile
[22] N. Copernicus Astronomical Center, Rabiańska 8, 87–100 Toruń, Poland